UCRL- 93869
PREPRINT

Received by OSTI

SEP 3 0 1986

Development of an X-Ray Framing Camera

UCRL--93869

DE86 016082

D. G. Stearns, J. D. Wiedwald,
W. M. Cook, and R. L. Hanks
Lawrence Livermore National Laboratory
Livemore, CA

This paper was prepared for the
6th Topical Conference on High
Temperature Plasma Diagnostics
Hilton Head Island, SC
3/9-13/86

3/5/86

Lawrence Livermore National Laboratory

DEVELOPMENT OF AN X-RAY FRAMING CAMERA*

D. G. Stearns, J. Wiedwald, B. M. Cook and R. Hanks

An essential requirement for the achievement of inertial confinement fusion using laser drivers is that the D-T fuel be compressed symmetrically with a minimum increase in entropy. Consequently it is important to study the hydrodynamics of fuel pellet implosions under realistic conditions, eg. non-uniform laser drivers and imperfect targets. An x-ray framing camera will allow the direct observation of hydrodynamic instabilities and asymmetries that can degrade the performance of a fuel pellet implosion. In a typical experiment, the imploding fuel pellet will be backlit with an intense laser-induced x-ray source, and the framing camera will record a radiograph of the implosion event through an x-ray microscope. When the frame duration is less than 100 ps, the image will be essentially be a "snapshot" of the pellet at a particular stage of compression. Hence the x-ray framing camera will be an ideal tool for diagnosing the dynamics of the implosion process.

We are presently developing an ultrafast x-ray framing camera, to be used in laser fusion experiments on the NOVA facility at LLNL. The framing camera will provide high-fidelity images with frame durations of less than 100 ps. The first prototype camera will generate a single image approximately one square centimeter in area, with a spatial resolution of ~30 microns at the image plane. Coupling the framing camera to a 22X Wolter x-ray microscope will provide resolution at the target of

*This work was performed under the auspices of the U.S. Department of Energy by Lawrence Livermore National Laboratory under contract No. W-7405-Eng-48.

~2 microns. The camera will be optically triggered using a laser pulse that is synchronous with the NOVA driver beams.

Design

The schematic design of the framing camera is shown in Figure 1. The x-ray image is incident on a transmission photocathode of CsI deposited on a 50-micron-thick beryllium window. The photocathode is incorporated into a suspended-strip transmission line. The suspended strip is fabricated by applying conductive ink to a substrate of machinable ceramic. The width of the strip is 25 mm and the gap between the strip and the ground plane is 1 mm, yielding a characteristic impedance for the transmission line of 15 ohms.

In the "off" state a reverse DC bias of 500 volts prevents the photoelectrons from leaving the surface of the photocathode. In order to record an image frame, a high-voltage gate pulse is generated and propagated across the photocathode. The voltage pulse is generated using a photoconductive switch mounted directly in the transmission line. We have fabricated and tested switches composed of semi-insulating gallium arsenide and silicon-on-sapphire, with gaps of both 1.5 mm and 2.5 mm. The photoconductive switch electrically isolates a charge-line section which is pulse-biased to -10 kV. The switch is activated with a short light pulse of moderate energy (~0.25 mJ) coupled in through a fiber optic light guide, producing a -5 kV gate pulse. The duration of the gate pulse is equal to twice the electrical length of the charge line and the rise time of the gate pulse corresponds to the temporal width of the trigger light pulse. The gate pulse propagates along the transmission line and is eventually dissipated in a thick-film resistor. The transmission line gap underneath the resistor decreases linearly to maintain a constant line impedance and hence suppress reflections.

During the time that the gate pulse traverses the photocathode, a photoelectron replica of the x-ray image is accelerated across the transmission line gap. A thin microchannel plate (12-micron-diameter channels, l/d=20) is mounted in the ground plane directly opposite the photocathode. The microchannel plate is not electrically biased, but serves only as a direction-sensitive filter, preventing the x-ray image that passes through the semi-transparent photocathode from being detected when the camera is in the "off" state, while transmitting the photoelectron image when the camera is gated "on". This is possible because the x-rays and the photoelectrons arrive at the microchannel plate at different angles of incidence. The framing camera is oriented so that the x-rays are incident normal to the photocathode and hence also to the microchannel plate. The photoelectrons, however, are deflected by the magnetic field of the transverse electromagnetic wave in the transmission line, and arrive at the microchannel plate at an average angle of 3.8 degrees. The channels of the microchannel plate are biased at 3.8 degrees from normal so that the photoelectrons pass through the plate while the x-rays are blocked.

The gated photoelectron image is directly recorded by a thinned charge-coupled device (CCD) positioned in close proximity

(0.5 mm) to the back surface of the microchannel plate. The CCD is the RCA SID501. Several of the most important operating parameters of this CCD are listed in Table 1. The device is thinned to eight microns, making it extremely sensitive to electron bombardment at the back surface (ie. the surface opposite the gate structure). The combination of a minimal dead layer and a low dark current at room temperature should provide sensitivity adequate to detect individual 4.5 keV electrons.

The anticipated performance specifications of the x-ray framing camera are listed in Table 2. The performance requirements are dictated by the applications to laser fusion experiments and a discussion of the issues can be found elsewhere (1). The most important features of the framing camera are the excellent spatial resolution, essentially limited by the 30 micron pixel size of the CCD, and the frame duration of less than 100 ps.

Characterization

The fabrication of the components of the first prototype x-ray framing camera is now essentially complete. The characterization of the individual components is presently in progress, and is discussed below. The assembly and testing of the prototype instrument will take place within the next year.

Gating Pulse Generation and Propagation

A crucial aspect of the successful operation of the framing camera is the ability to generate and propagate high voltage pulses of short duration and minimal spatial variation along the transmission line. The duration of the pulse determines the temporal resolution of the camera. The variation of the voltage along the transverse dimension of the transmission line affects the fidelity of the image. In order to unambiguously study the performance of the transmission line it is necessary to be able to map out the electromagnetic field inside the line both spatially and temporally on the picosecond timescale. This is achieved by using electro-optical sampling.

We have built the electro-optic sampling system shown in Figure 2, based upon the original experiment of Valdmanis et al. (2). A synchronously-pumped mode-locked dye laser is amplified to provide ~8 ps pulses of energy ~1 mJ/pulse at a wavelength of 610 nm and a repetition rate of 10 Hz. Most of the light pulse is coupled into the fiber optic light guide and used to activate the photoconductive switch. The light intensity inside the light guide can be as high as 10^9 W/cm^2. At this intensity we have measured a throughput efficiency of 50% and no appreciable temporal broadening of the light pulse. The charge line is pulse-biased to 2 kV, which is the maximum voltage that the charge line can sustain in air without electrical breakdown. When the photoconductive switch is illuminated an approximately 1 kV pulse of short duration is generated and propagates along the transmission line. A small fraction of the laser pulse is split off and used to sample the electric field inside the transmission line. This is achieved by linearly polarizing the light and focussing it through a small lithium tantalate crystal that is suspended in the transmission line gap. The polarization of the light rotates an amount proportional to the instantaneous electric field strength inside the birefringent crystal. The rotation of the polarization is analyzed by measuring the individual components of the polarization with two photo-diode detectors. Temporal scans are made by varying the relative delay between the firing of the photoconductive switch and the probing of the lithium tantalate crystal. The entire transmission line is mounted on x and y stages so that spatial scans are accomplished by translating the transmission line about the fixed position of the crystal. The temporal resolution of the sampling system is determined by the convolution of the light pulse width and the transit time through the crystal, to yield in this case a resolution of 11 ps. The spatial resolution is 0.5 mm, determined by the size of the crystal.

The electro-optic sampling system has been used to study the behavior of the framing camera transmission line, complete with an in-line photocathode and microchannel plate. Figure 3 shows a two-dimensional spatial scan of the voltage pulse at the instant in time at which the pulse is centered at the position of the photocathode. The electric field is observed to be strongly confined to the interior region of the transmission line. The field appears to be reasonably uniform across the transverse dimension of the waveguide, exhibiting variations at the 10-20% level. Temporal scans of the voltage pulse are shown in Figure 4. These scans were measured at the center of the transmission line at various positions downstream from the photoconductive switch. It is evident that the pulse propagates with minimal attenuation and dispersion, which demonstrates that the photocathode and microchannel plate do not adversely affect the electrical properties of the transmission line.

An unexpected feature observed in this experiment is that the voltage pulse exhibits a significant amount of ringing at a characteristic frequency of approximately 40 GHz. The ringing is attributed to LC oscillations that arise from the capacitance and inductance of the photoconductive switch. The switch can be modeled as a simple lumped circuit of a capacitance and an inductance in parallel. By comparing the theoretical response with the experimentally measured gate pulses we infer values for the switch capacitance and inductance of C=0.8pF and L=20pH respectively. These values are consistent with the dimensions and geometry of the switch. Physically, the ringing arises because the capacitance of the photoconductive switch prevents the initial distribution of charge on the charge line from being uniform. The effect of the oscillations on the performance of the framing camera, however, is not serious. The trajectory of any particular photoelectron is determined by the electromagnetic force on the electron, integrated over the approximately 40 ps transit time of the electron across the transmission line gap. Computer calculations show that the integrating effect of the transit time significantly suppresses the effect of the voltage pulse oscillations on the photoelectron trajectories.

Microchannel Plate Throughput

The successful operation of the framing camera requires that the microchannel plate perform as an extremely efficient direction-sensitive filter. Photoelectrons with trajectories at four degrees from normal must pass through the microchannel plate, while the ungated x-ray signal at normal incidence must be strongly attenuated. We have tested the x-ray throughput of the microchannel plate in the following experiment. The microchannel plate was mounted in a vacuum chamber, in a manipulator that allowed rotations about an axis normal to the surface of the plate (phi) and an axis in the plane of the plate (theta). A collimated x-ray source was incident on the front surface of the microchannel plate and a proportional gas counter directly behind the plate was used to measure the throughput. The entire manipulator could be moved out of the x-ray beam in order to measure the incident x-ray flux, and hence make absolute throughput measurements.

The throughput at x-ray energies of 2.0 and 4.5 keV is shown in Figure 5 as a function of the angles phi and theta. It is apparent in Figure 5a that the x-ray throughput has a relatively broad maximum as a function of phi. It is also evident that the throughput away from the maximum is greater at lower energies, probably due to critical angle reflection of the x-rays off the walls of the microchannels. The x-ray throughput as a function of theta is shown on a logarithmic scale in Figure 5b. The transmission peaks at 3.8 degrees from the normal, corresponding to the bias angle of the channels. The maximum observed throughput of 50% is close to the theoretical value of 55%, calculated from the ratio of open surface area to total surface area. The x-ray throughput decreases strongly at angles away from the maximum, such that the attenuation is greater than four orders of magnitude for x-rays at normal incidence. This indicates that the microchannel plate can indeed perform as an effective x-ray attenuator in the framing camera.

Work in Progress

Several important experiments are currently in progress that will complete the characterization of the individual components of the framing camera. We are in the process of measuring the photoelectron throughput of the microchannel plate, as well as the photoelectric emission due to the absorption of x-rays by the microchannel plate. Photoelectrons emitted from the microchannel plate are a potential source of noise and must be suppressed. We are also presently setting up a facility to thoroughly characterize the response of the RCA SID501 CCD to direct electron bombardment.

The evaluation of the individual components should be completed within the next year, at which time the first prototype camera will be assembled and tested as a unit.

REFERENCES

1) 1984 Laser Program Annual Report, Lawrence Livermore National Laboratory, Livermore, Calif., UCRL-50021-84 (1985), pp. 5-57 to 5-60.

2) J. A. Valdmanis, G. Mourou and C. W. Gabel, Appl. Phys. Lett., 41, (1982) 211.

TABLES

1) Operating parameters of the RCA SID501 charge-coupled device.

2) Anticipated performance specifications of the x-ray framing camera.

FIGURES

1) A schematic representation of the x-ray framing camera.

2) The configuration of the electro-optic sampling system.

3) A two-dimensional spatial scan of the high voltage gate pulse inside the transmission line, at the instant in time at which the pulse is centered at the position of the photocathode. The measurement is made using the electro-optic sampling technique.

4) Temporal scans of the high voltage gate pulse measured at several positions along the transmission line. The positions refer to the distance from the photoconductive switch. The origins of the time axes have been chosen to facilitate comparison.

5) X-ray transmission through the microchannel plate as a function of the orientation of the plate. Maximum throughput occurs when the channels are aligned with the direction of x-ray propagation ($\phi = 0^\circ$, $\theta = 3.75^\circ$), whereas the transmission is strongly attenuated for x-rays at normal incidence ($\theta = 0^\circ$).

CCD specifications

Pixel array size	512 X 320
Pixel size	30 X 30 μm
Total image area	15.36 X 9.6 mm
Output noise	50 e^- + thermal
Dark current	1.5 nA (approximately)
Full well capacity	600,000 electrons
Dead layer	<1 keV (est)

20-10-0286-0940

Framing camera performance

Image size	~1 × 1 cm
Spatial resolution (at image plane)	18 lp/mm (50% modulation)
Temporal resolution	~50 ps
Dynamic range	>100:1
Sensitivity	Single photon (1–10 keV)
Quantum efficiency	1–10% (1–10 keV)
Shutter efficiency	$>10^4$

20-01-0286-0941

X-ray framing camera

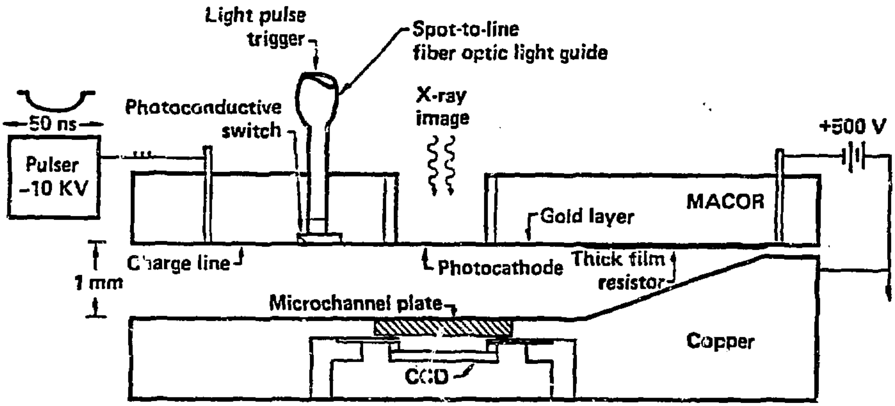

20-01-0286-0938

Electro-optic sampling system

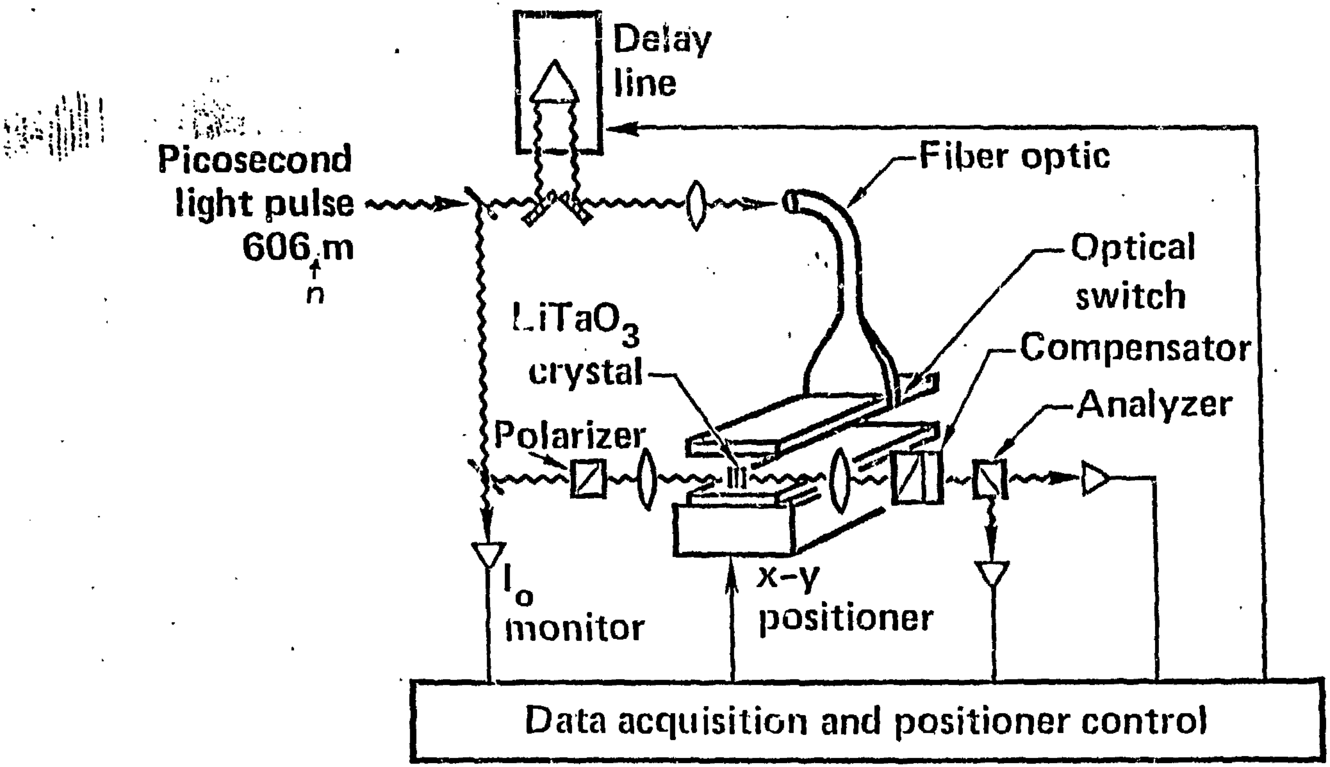

20-01-1085-5017

High voltage gate pulse

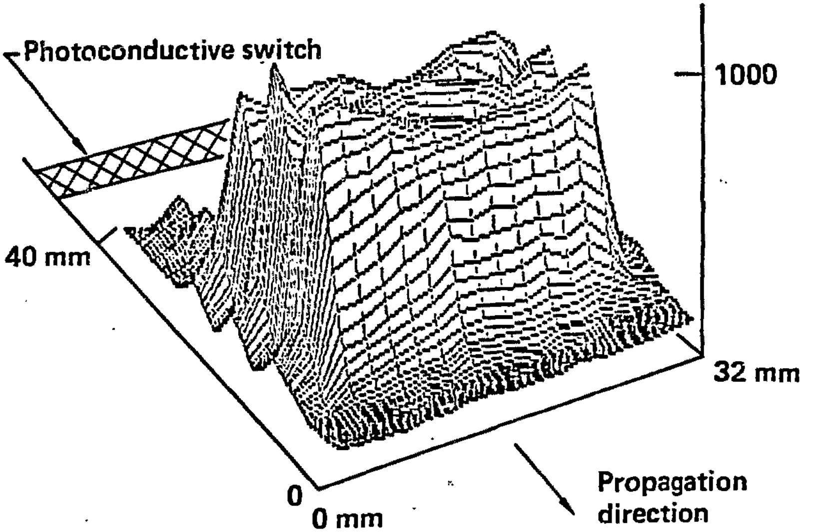

20-01-0286-0943

Gate pulse dispersion

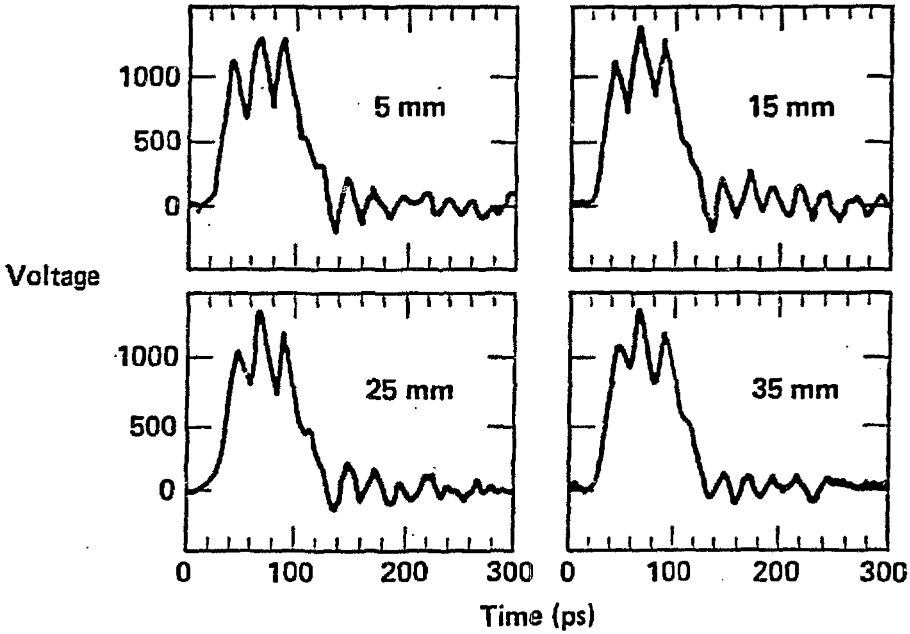

20-01-0286-0939

X-ray transmission measurements

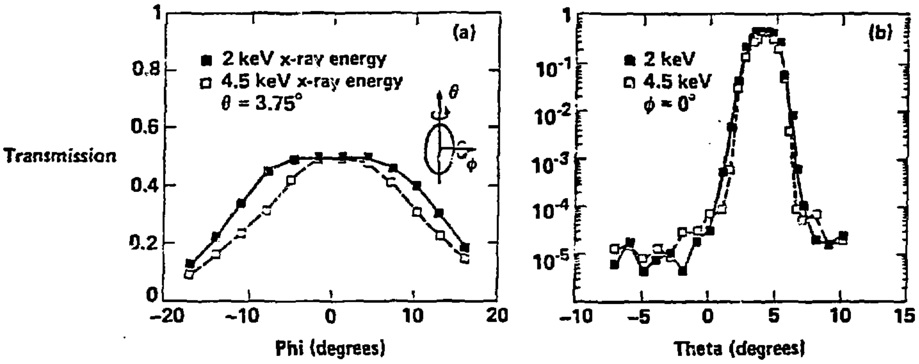

20-01-0286-0942